Diborenes

DOI: 10.1002/anie.201311110

Boron Radical Cations from the Facile Oxidation of Electron-Rich Diborenes**

Philipp Bissinger, Holger Braunschweig, Alexander Damme, Thomas Kupfer, Ivo Krummenacher, and Alfredo Vargas*

Dedicated to Professor Helmut Werner on the occasion of his 80th birthday

Abstract: *The realization of a phosphine-stabilized diborene, $Et_3P{\cdot}(Mes)B{=}B(Mes){\cdot}PEt_3$ (**4**), by KC_8 reduction of $Et_3P{\cdot}B_2Mes_2Br_2$ in benzene enabled the evaluation and comparison of its electronic structure to the previously described NHC-stabilized diborene IMe·(Dur)B=B(Dur)·IMe (**1**). Importantly, both species feature unusual electron-rich boron centers. However, cyclic voltammetry, UV/Vis spectroscopy, and DFT calculations revealed a significant influence of the Lewis base on the reduction potential and absorption behavior of the B–B double bond system. Thus, the stronger σ-donor strength and larger electronegativity of the NHC ligand results in an energetically higher-lying HOMO, making **1** a stronger neutral reductant as **4** (**1**: $E_{1/2} = -1.55$ V; **4**: −1.05 V), and a smaller HOMO–LUMO gap of **1** accompanied by a noticeable red-shift of its lowest-energy absorption band with respect to **4**. Owing to the highly negative reduction potentials, **1** and **4** were easily oxidized to afford rare boron-centered radical cations (**5** and **6**).*

Recent research in main-group-element chemistry has focused more and more on the realization of homoatomic multiple bonding between elements other than carbon.[1] However, when it comes to boron, examples are rare, which is related to the inherent electron deficiency of the boron nucleus. Thus, B–B multiple bonding was first realized by populating the empty π orbital at boron through reduction of suitable diboranes(4) to afford a few radical-anionic and dianionic species (Figure 1).[2] Furthermore, theoretical studies also suggested a certain stability of neutral B–B double and triple bond species.[3] However, it required enormous experimental efforts and Lewis base stabilization to eventually succeed in the realization of such compounds. Thus, the highly reactive H–B=B–H moiety has been isolated by Robinson as its doubly base-stabilized derivative using *N*-heterocyclic carbene (NHC) ligands (Figure 1).[4] Here, NHC·(H)B=B(H)·NHC (NHC = IDip = 1,3-bis(2,6-diisopropylphenyl)imidazol-2-ylidene; or NHC = IMes = 1,3-bis(2,4,6-trimethylphenyl)imidazol-2-ylidene) are formed in relatively low yields by hydrogen abstraction from the reaction media. Furthermore, the reductive coupling of $NHC{\cdot}BBr_3$ suffered from the formation of side products, such as $NHC{\cdot}(H)_2B{-}B(H)_2{\cdot}NHC$. Recently, we developed an improved and more general procedure to access neutral base-stabilized diborenes, employing sterical demanding aryl substituents at boron.[5] Thus, reduction of $IMe{\cdot}BRCl_2$ (IMe = 1,3-dimethylimidazol-2-ylidene) enabled the isolation of IMe·(R)B=B(R)·IMe (**1**: R = Dur = 2,3,5,6-tetramethylphenyl; **2**: R = Mes = 2,4,6-trimethylphenyl) in high yields (Figure 1). Initial studies on the reactivity of the B–B double bond highlighted its electron richness facilitating the olefin-type side-on coordination to AgCl.

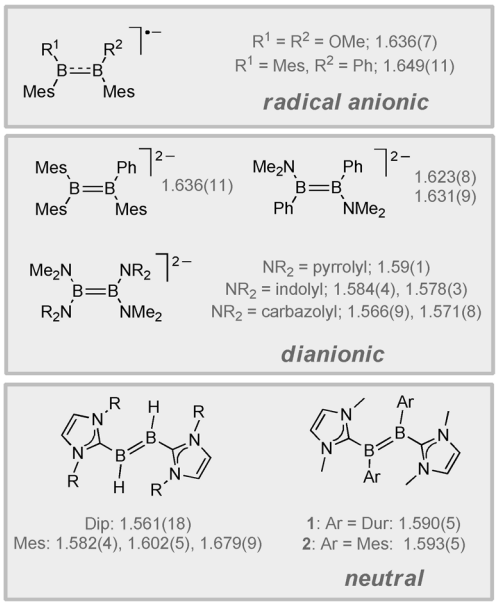

Figure 1. Examples of B–B multiple bonding with experimentally (X-ray) determined B–B distances [Å].

Some other, but limited approaches towards B–B multiple bonding include: a) Matrix isolation of OC·BB·CO upon reaction of laser-vaporized boron atoms with CO;[6] b) Reduction of NHC-stabilized diborane $IDip{\cdot}(Br)_2B{-}B(Br)_2{\cdot}IDip$ with a preformed B–B single bond; thus either the diborene IDip·(Br)B=B(Br)·IDip or the first room

[*] Dr. P. Bissinger, Prof. Dr. H. Braunschweig, Dr. A. Damme, Dr. T. Kupfer, Dr. I. Krummenacher
Institut für Anorganische Chemie, Julius-Maximilians-Universität Würzburg
Am Hubland, 97074 Würzburg (Germany)
E-mail: h.braunschweig@uni-wuerzburg.de
Dr. A. Vargas
Department of Chemistry, School of Life Sciences, University of Sussex
Brighton BN1 9QJ, Sussex (UK)

[**] This work was supported by the Deutsche Forschungsgemeinschaft.
Supporting information for this article is available on the WWW under http://dx.doi.org/10.1002/anie.201311110.

temperature stable diboryne IDip·BB·IDip were produced depending on the reaction stoichiometry;[7] c) Generation of the B–B double bond in the coordination sphere of a transition metal. In $[(Et_3P)_2Pt\{B_2(Dur)_2\}]$, the diborene fragment remains coordinated to platinum for which reason no further Lewis base stabilization of the B=B system is required.[8]

Interestingly, all attempts to transfer the reductive coupling approach to related phosphine-stabilized precursors consistently failed so far. Furthermore, no suitable doubly phosphine-stabilized diborane(4) precursors are known, which also hampers the isolation of such species. Rather it was demonstrated that 1,2-diaryl-1,2-dihalodiboranes(4) react even with an excess of phosphine PR_3 to yield 1:1 sp^2–sp^3 diborane adducts.[9] Here, either the formation of simple adducts with a bridging halide (type a) or a rearrangement process affording 1,1′-diaryl-2,2′-dihalodiborane(4) adducts (type b) is the preferred reaction pathway, depending on the sterical requirements of the phosphine ligand. Although such diboranes(4) do not coordinate a second equivalent of the Lewis base to form $R_3P{\cdot}(R)_2B{-}B(R)_2{\cdot}PR_3$, we reasoned that type a species might be suitable candidates for the realization of neutral bisphosphine-stabilized diborenes, if additional Lewis base is offered in situ.

To this end, $Et_3P{\cdot}B_2MeS_2Br_2$ (**3**) was reduced with excess KC_8 in benzene solution in the presence of PEt_3 (Scheme 1).[10] As anticipated, reduction afforded the

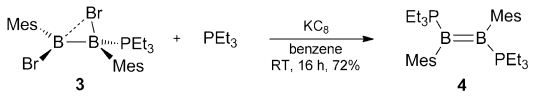

Scheme 1. Synthesis of **4**.

bisphosphine-stabilized diborene **4** as a yellow solid in 72% yield of isolated product. The ^{11}B NMR signal of **4** in C_6D_6 ($\delta = 16.3$ ppm) is somewhat shifted to higher field upon changing the Lewis base from NHC to phosphine (cf. **1** $\delta =$ 24.7 ppm, **2** $\delta = 24.1$ ppm, IDip·(H)B=B(H)·IDip $\delta =$ 25.3 ppm).[4a,5] Direct comparison to other three-coordinate boron phosphine adducts turned out difficult due to the lack of suitable examples in the literature. The PMe_3 adduct of borabenzene, $(C_5H_5B){\cdot}PMe_3$, most likely approximates the bonding situation of **4** best, and its ^{11}B NMR chemical shift ($\delta = 20.8$ ppm) is thus quite similar.[11] However, the presence of a B–B double bond is clearly evident in the molecular structure of **4** in the solid state.[12] Thus, the boron atoms of **4** adopt trigonal planar geometries ($\Sigma_B = 360°$) with a B–B distance (1.579(3) Å) comparable to those observed for NHC-stabilized diborenes IDip·(H)B=B(H)·IDip (1.561(18) Å), **1** (1.590(5) Å) and **2** (1.593(5) Å).[4a,5] The increase in B–B bond order comes along with a shortening/strengthening of the B–P bonds in **4** (1.9179(15) Å) as compared to the starting material **3** (1.996(2) Å).[9] A short B–P bond was also reported for the related $(C_5H_5B){\cdot}PMe_3$ system (1.900(8) Å).[11]

Having two similar diborene systems (**1** and **4**) to hand, we set out to evaluate their electronic structures in more detail. Cyclic voltammetry in THF revealed a single reversible oxidation event for **4** at −1.05 V, while two oxidation processes are visible in the case of **1**, the first one being reversible (−1.55 V) and the second being irreversible and leading to decomposition at a potential of −0.50 V.[10,12] These high reduction potentials are remarkable, keeping the inherent electron deficiency of boron in mind and are amongst the highest observed for neutral molecules, which illustrates well the electron richness of the B–B double bond system.[13] It should also be emphasized that this is a very rare case of a boron-centered radical cation,[14] and we are only aware of one other example, which was reported by Bertrand.[15] However, there is a surprisingly large difference of 0.5 V between the reduction potentials of **1** and **4**, with the NHC-substituted diborene **1** being a much stronger reductant than its phosphine analogue **4**. This finding indicates that the HOMO of **1** lies significantly higher in energy than that of **4**, which can be approximated by CV to 0.5 eV.[16] Results of DFT calculations clearly validate this picture providing an energy separation of 0.38 eV between the HOMOs of **1** (−3.15 eV) and **4** (−3.53 eV; as based on orbital eigenvalues depicted in Figure 2). Figure 2 also shows that the HOMOs of

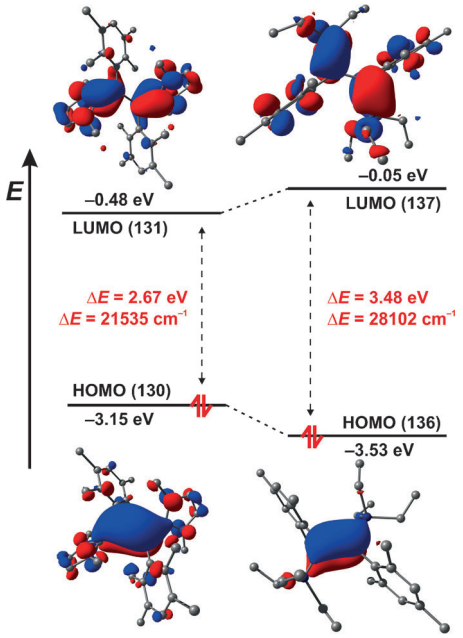

Figure 2. Frontier molecular orbitals and their respective energies of diborenes **1** (left) and **4** (right).

both diborenes are almost exclusively associated with the B–B π system. Thus, we suggest that it is the larger σ donor strength of the NHC ligand with respect to PEt_3 that leads to a higher electron density at the B–B double bond in **1**, thus raising the HOMO in energy relative to **4**.

Another difference in the electronic structures of **1** and **4** is evident in their UV/Vis spectra in Et_2O solution.[10,12] As described earlier, diborene **1** features three distinct absorption bands at $\lambda_{max} = 299$, 463, and 538 nm, which were assigned on the basis of time-dependent DFT calculations to transitions mainly arising from the B–B π system to ligand-

centered molecular orbitals ($\lambda_{calc} = 320$ nm: HOMO−1→LUMO; $\lambda_{calc} = 436$ nm: HOMO→LUMO + 1; $\lambda_{calc} = 519$ nm: HOMO→LUMO).[5] In contrast, phosphine-stabilized diborene **4** only shows two broad absorption bands in its UV/Vis spectrum at $\lambda_{max} = 366$ nm and 403 nm with the lowest energy transition significantly shifted to higher energies (ΔE 6567 cm^{-1}). TD DFT revealed that these absorptions are much more complicated in nature and involve different electronic excitations each consisting of a series of transitions all emanating from the B–B-centered HOMO into different virtual MOs. Accordingly, the absorptions at $\lambda_{max} = 366$ nm ($\lambda_{calc} = 319$, 346, 361 nm) and $\lambda_{max} = 403$ nm ($\lambda_{calc} = 401$, 412, 423 nm) each consist of three distinct excitations. At this point, we also puzzled why the HOMO–LUMO gap of **1** is obviously that much smaller than that of **4**. To address this question, we first evaluated the energies and shapes of the involved molecular orbitals of **1** and **4** by DFT methods (Figure 2). The calculations reproduced the observed experimental UV/Vis data very well, thus confirming a much larger HOMO–LUMO gap for **4** (3.48 eV; cf. **1**: 2.67 eV). Here, as already described in the CV discussion, the HOMO of **4** is lower in energy than the HOMO of **1** (ΔG 0.38 eV), while its LUMO is higher in energy (ΔG 0.43 eV). Furthermore, the calculations showed the HOMOs of **1** and **4** to be associated with the B–B π bonding interaction and the LUMOs to be mainly ligand-centered. Consequently, we reasoned that the large differences observed upon electronic excitation are a result of two different effects: The presence of a) an energy-rich HOMO of diborene **1** due to the larger σ donor strength of the NHC ligand; and b) a high-lying ligand-centered LUMO in **4**, which is presumably related to the lower electronegativity of the phosphorus center (P vs. C).

Next, we tried to assess the radical cationic species observed in the CV measurements experimentally by selective chemical oxidation of **1** and **4** by $(C_7H_7)BAr^f_4$ ($Ar^f = 3,5\text{-}(CF_3)_2\text{-}C_6H_3$). $(C_7H_7)BAr^f_4$ was considered a suitable oxidant because of its low oxidation potential, which also only produces an innocent and easy to remove by-product ($C_{14}H_{14}$), and also features a weakly coordinating anion thus providing stability and solubility. Reactions of **1** and **4** with $(C_7H_7)BAr^f_4$ occurred readily in Et_2O at room temperature, and the radical cations **5** and **6** were eventually isolated as purple (**5**: 71%) and green crystalline solids (**6**: 72%), respectively (Scheme 2).[10] Removal of one electron from the bonding π orbital between the two boron atoms results in a formal bond order of 1.5 for the radical cations **5** and **6**, which is also evident in their crystal structures.[10,12] Thus, the B–B distances of **5** (1.636(4) Å) and **6** (1.631(6) Å) are elongated with respect to their precursors (**1**: 1.590(5) Å; **4**: 1.579(3) Å), while the planarity of the boron centers remains unaffected by the lower bond order (**5**: $\Sigma_{B1} = 359.85°$, $\Sigma_{B2} = 360.01°$; **6**: $\Sigma_{B1} = 359.85°$, $\Sigma_{B2} = 360.01°$).[5]

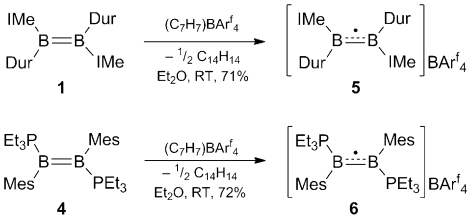

Scheme 2. Syntheses of **5** and **6**.

In the continuous-wave X-band EPR spectra of diethyl ether solutions of the two radical cations, the resonances are only poorly resolved, even at low concentrations around the detection limit. While radical **5** displays a single broad resonance at g_{iso} 2.0027, the spectrum of **6** exhibits a 1:2:1 triplet owing to the coupling of the unpaired electron with two equivalent phosphorus atoms (g_{iso} 2.0024; $A(^{31}P)$ 21 G; Figure 3). In both cases, the lack of an observable boron

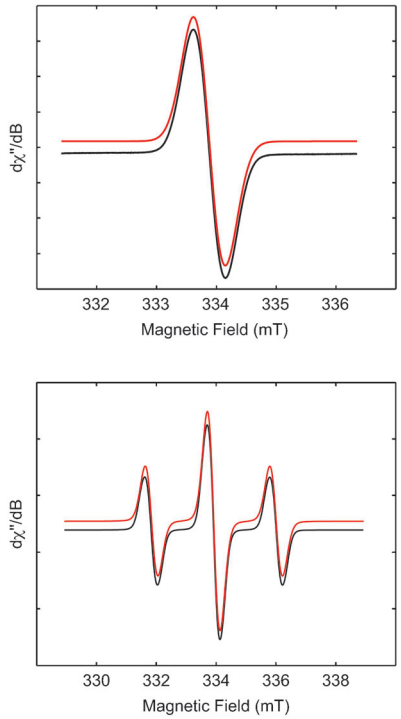

Figure 3. Experimental (black) and simulated (red) X-band (9.38 GHz) EPR spectra of **5** (top) and **6** (bottom) in Et_2O solution.

hyperfine coupling, which can be approximated from the EPR line widths to be smaller than 1 G, suggests a rather small amount of unpaired spin density on the boron atoms.

The electronic structure of radical cations **5** and **6** was also elucidated by a combination of UV/Vis spectroscopy (Et_2O; Figure 4) and TD DFT calculations.[10] The results of these studies are analogous to that obtained for the neutral diborene precursors **1** and **4**. Thus, removal of one electron from the HOMOs of **1** and **4** by oxidation does not alter the shape of the resulting molecular orbitals, and the SOMOs of **5** and **6** are still of pure B–B π bonding character.[12] The UV/Vis spectrum of NHC-substituted radical cation **5** features seven absorption bands between $\lambda_{max} = 270$ nm and 503 nm, with the main absorptions being at $\lambda_{max} = 340/367$ nm and 445/503 nm. These absorption bands are quite well reproduced by the calculations. Here, excitations were found at $\lambda_{calc} = 509$ nm and 468 nm, which consist of SOMO(α)→LUMO(α)/HOMO−1(β)→SOMO(β) and HOMO−4(β)→SOMO(β)

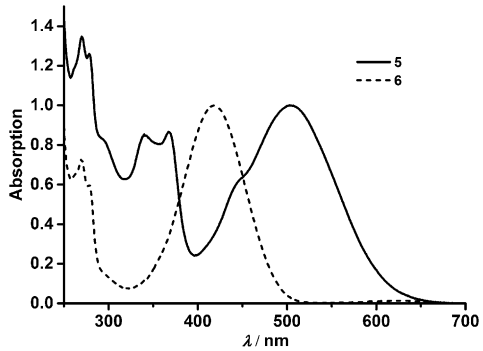

Figure 4. UV/Vis spectra of radical cations **5** and **6** in Et_2O.

transitions, respectively. The absorption band at $\lambda_{calc} = 362$ nm is far more complex and associated with 19 transitions, the main components being SOMO(α)→LUMO + 1(α) and HOMO−3(α)→LUMO(α). By contrast, the UV/Vis spectrum of **6** is quite simple showing only one major absorption band at $\lambda_{max} = 419$ nm, which is easily assigned to the SOMO(α)→LUMO(α) excitation ($\lambda_{calc} = 384$ nm). Similar to their neutral precursors, the lowest energy absorption of the NHC-stabilized radical cation **5** occurs at significantly lower energy than that of its phosphine analogue **6** (ΔE 4938 cm^{-1}), which is again a result of an energetically high-lying SOMO in **5** (ΔG 0.73 eV) and LUMO in **6** (ΔG 0.21 eV), respectively. Consequently, the SOMO–LUMO gap is larger for **6** (4.16 eV; cf. **5**: 3.22 eV)

With the synthesis of phosphine-stabilized diborene **4**, we were able to significantly expand the chemistry of diborenes. Thus, we have shown that a) not only NHC coordination can lead to stable diborenes and that b) the experimental access is not limited to reductive coupling approaches. Furthermore, we have provided quantified evidence for the unusual electron richness of the B=B double bond, which is highlighted by highly negative reduction potentials. Accordingly, removal of one electron from the B=B double bond of diborenes **1** and **4** occurred readily to afford stable radical cations **5** and **6**. Having two different systems in hand, a more detailed evaluation of the electronic structure became possible, and we found that the nature of the stabilizing Lewis base exerts a strong influence. Thus, changing the Lewis base from NHC (**1**, **5**) to phosphine (**4**, **6**) entails a) a significant decrease in the reduction potential of the diborenes ($\Delta E_{1/2}$ 0.5 V) and b) an increase of the HOMO–LUMO (ΔE 6567 cm^{-1}) and SOMO–LUMO gap (ΔE 4938 cm^{-1}), respectively. Experiments regarding the reactivity and applicability of theses neutral and radical cationic species are a major part of current research in our laboratories.

Received: December 23, 2013
Revised: March 4, 2014
Published online: April 7, 2014

Keywords: diborane · diborene · oxidation · radical cation · reduction

[1] a) Y. Wang, G. H. Robinson, *Chem. Commun.* **2009**, 5201 – 5213; b) R. C. Fischer, P. P. Power, *Chem. Rev.* **2010**, *110*, 3877 – 3923; c) Y. Wang, Y. Xie, M. Y. Abraham, P. Wei, H. F. Schaefer, P. von R. Schleyer, G. H. Robinson, *Chem. Commun.* **2011**, *47*, 9224 – 9226; d) Y. Wang, Y. Xie, P. Wei, R. B. King, H. F. Schaefer, P. von R. Schleyer, G. H. Robinson, *Science* **2008**, *321*, 1069 – 1071; e) R. West, M. J. Fink, J. Michl, *Science* **1981**, *214*, 1343 – 1344; f) P. J. Davidson, D. H. Harris, M. F. Lappert, *J. Chem. Soc. Dalton Trans.* **1976**, 2268 – 2274; g) N. A. Piro, J. S. Figueroa, J. T. McKellar, C. C. Cummins, *Science* **2006**, *313*, 1276 – 1279; h) A. Sekiguchi, R. Kinjo, M. Ichinohe, *Science* **2004**, *305*, 1755 – 1757; i) J. Su, X.-W. Li, R. C. Crittendon, G. H. Robinson, *J. Am. Chem. Soc.* **1997**, *119*, 5471 – 5472.

[2] a) A. Berndt, H. Klusik, K. Schlüter, *J. Organomet. Chem.* **1981**, *222*, c25 – c27; b) H. Klusik, A. Berndt, *Angew. Chem.* **1981**, *93*, 903 – 904; *Angew. Chem. Int. Ed. Engl.* **1981**, *20*, 870 – 871; c) W. J. Grigsby, P. P. Power, *Chem. Commun.* **1996**, 2235 – 2236; d) W. J. Grigsby, P. Power, *Chem. Eur. J.* **1997**, *3*, 368 – 375; e) A. Moezzi, M. M. Olmstead, P. P. Power, *J. Am. Chem. Soc.* **1992**, *114*, 2715 – 2717; f) A. Moezzi, R. A. Bartlett, P. P. Power, *Angew. Chem.* **1992**, *104*, 1075 – 1076; *Angew. Chem. Int. Ed. Engl.* **1992**, *31*, 1082 – 1083; g) H. Nöth, J. Knizek, W. Ponikwar, *Eur. J. Inorg. Chem.* **1999**, 1931 – 1937; h) H. Braunschweig, R. D. Dewhurst, *Angew. Chem.* **2013**, *125*, 3658 – 3667; *Angew. Chem. Int. Ed.* **2013**, *52*, 3574 – 3583.

[3] a) E. Kaufmann, P. von R. Schleyer, *Inorg. Chem.* **1988**, *27*, 3987 – 3992; b) A. Papakondylis, E. Miliordos, A. Mavridis, *J. Phys. Chem. A* **2004**, *108*, 4335 – 4340; c) L. C. Ducati, N. Takagi, G. Frenking, *J. Phys. Chem. A* **2009**, *113*, 11693 – 11698; d) M. P. Mitoraj, A. Michalak, *Inorg. Chem.* **2011**, *50*, 2168 – 2174; e) N. Holzmann, A. Stasch, C. Jones, G. Frenking, *Chem. Eur. J.* **2011**, *17*, 13517 – 13525; f) S.-D. Li, H.-J. Zhai, L.-S. Wang, *J. Am. Chem. Soc.* **2008**, *130*, 2573 – 2579.

[4] a) Y. Wang, B. Quillian, P. Wei, C. S. Wannere, Y. Xie, R. B. King, H. F. Schaefer, P. von R. Schleyer, G. H. Robinson, *J. Am. Chem. Soc.* **2007**, *129*, 12412 – 12413; b) Y. Wang, B. Quillian, P. Wei, Y. Xie, C. S. Wannere, R. B. King, H. F. Schaefer, P. von R. Schleyer, G. H. Robinson, *J. Am. Chem. Soc.* **2008**, *130*, 3298 – 3299.

[5] P. Bissinger, H. Braunschweig, A. Damme, T. Kupfer, A. Vargas, *Angew. Chem.* **2012**, *124*, 10069 – 10073; *Angew. Chem. Int. Ed.* **2012**, *51*, 9931 – 9934.

[6] M. Zhou, N. Tsumori, Z. Li, K. Fan, L. Andrews, Q. Xu, *J. Am. Chem. Soc.* **2002**, *124*, 12936 – 12937.

[7] H. Braunschweig, R. D. Dewhurst, K. Hammond, J. Mies, K. Radacki, A. Vargas, *Science* **2012**, *336*, 1420 – 1422.

[8] H. Braunschweig, A. Damme, R. D. Dewhurst, A. Vargas, *Nat. Chem.* **2013**, *5*, 115 – 121.

[9] a) H. Braunschweig, A. Damme, J. O. C. Jimenez-Halla, T. Kupfer, K. Radacki, *Angew. Chem.* **2012**, *124*, 6372 – 6376; *Angew. Chem. Int. Ed.* **2012**, *51*, 6267 – 6271; b) H. Braunschweig, A. Damme, R. D. Dewhurst, T. Kupfer, K. Radacki, E. Siedler, A. Trumpp, K. Wagner, C. Werner, *J. Am. Chem. Soc.* **2013**, *135*, 8702 – 8707.

[10] Experimental, spectroscopic, crystallographic, and computational details are given in the Supporting Information.

[11] D. A. Hoic, J. R. Wolf, W. M. Davis, G. C. Fu, *Organometallics* **1996**, *15*, 1315 – 1318.

[12] Figure for the crystal structures of **4**–**6**, CVs of **1** and **4**, UV/Vis spectra of **4**–**6**, as well as graphical representations of the frontier molecular orbitals of the radical cations **5** and **6** are given in the Supporting Information.

[13] a) H. S. Farwaha, G. Bucher, J. A. Murphy, *Org. Biomol. Chem.* **2013**, *11*, 8073 – 8081; b) N. G. Connelly, W. E. Geiger, *Chem. Rev.* **1996**, *96*, 877 – 910.

[14] See, for example: a) C. D. Martin, M. Soleilhavoup, G. Bertrand, *Chem. Sci.* **2013**, *4*, 3020 – 3030; b) D. P. Curran, A. Solovyev, M. M. Brahmi, L. Fensterbank, M. Malacria, E. Lacôte, *Angew. Chem.* **2011**, *123*, 10476 – 10500; *Angew. Chem. Int. Ed.* **2011**, *50*, 10294 – 10317; c) J. C. Walton, M. M. Brahmi, L. Fensterbank, E. Lacôte, M. Malacria, Q. Chu, S.-H. Ueng, A. Solovyev, D. P. Curran, *J. Am. Chem. Soc.* **2010**, *132*, 2350 – 2358.

[15] R. Kinjo, B. Donnadieu, M. A. Celik, G. Frenking, G. Bertrand, *Science* **2011**, *333*, 610 – 613.

[16] The energies of the HOMOs of **1** and **4** were approximated by the formula $E_{HOMO} = -[E(Fc/Fc^{+}) + 5.1]$ (eV). C. M. Cardona, W. Li, D. Stockdale, G. C. Bazan, *Adv. Mater.* **2011**, *23*, 2367 – 2371.

